RSC Advances

PAPER

View Article Online
View Journal | View Issue

Cite this: *RSC Adv.*, 2017, **7**, 35619

The synergistic effect of cuprous oxide on an intumescent flame-retardant epoxy resin system

Ming-Jun Chen,* Xu Wang, Xin-Lei Li, Xing-Ya Liu, Liu Zhong, Hui-Zhen Wang and Zhi-Guo Liu*

Neat epoxy resin (EP) is a highly flammable material, and the pyrolysis volatiles of it contain some harmful gases such as carbon monoxide, aromatic compounds, hydrocarbons, *etc.* Herein, an organic–inorganic hybrid named ethanediamine-modified ammonium polyphosphate (EDA-APP) was used to prepare monocomponent intumescent flame-retardant EP composites. Cu_2O was used as a synergist for the EP/EDA-APP system. The fire behavior and smoke emission of EP composites were evaluated by limiting oxygen index (LOI), UL-94 vertical burning, and cone calorimeter test. The results show that the minimum demand of EDA-APP (21 wt%) is lower than that of APP (25 wt%) to obtain a UL-94 V-0 rating. In addition, the contents of EDA-APP can be further reduced to 16.3 wt% to reach UL-94 V-0, and a high LOI value of 31% can be obtained only *via* the addition of extra 1.7 wt% Cu_2O. Interestingly, the total smoke production (TSP) and carbon monoxide production (COP) are further decreased by loading Cu_2O onto the EP/EDA-APP composite. Then, the thermal decomposition behavior, morphology, and composition of EP composites and their condensed and gaseous pyrolysis products were analyzed by thermogravimetric analysis (TGA), scanning electron microscopy (SEM), Fourier transform infrared spectroscopy (FTIR), and energy-dispersive X-ray (EDX) spectroscopy, respectively. The test results revealed that the enhancement in flame retardancy and smoke suppression of EP/EDA-APP/Cu_2O is due to the synergistic effect and catalytic action of Cu_2O for accelerating the char formation rate and improving the formation amount, intumescent degree, and compactness of char.

Received 15th May 2017
Accepted 3rd July 2017

DOI: 10.1039/c7ra05482c

rsc.li/rsc-advances

1 Introduction

The flammability of epoxy resin (EP) is its potential fire hazard. When it is ignited, the fire rapidly spreads, and great volumes of toxic fumes, such as those of carbon monoxide, aromatic compounds, hydrocarbons, *etc.* will be concomitantly released.[1,2] This adversely affects human body and environment and also makes firefighting very difficult.[3] Therefore, it is an urgent social demand to endow EP with good flame retardancy and smoke suppression.

In recent years, ammonium polyphosphate (APP) is one of the most widely used halogen-free flame retardants. This is because it provides both acid and gas sources for the intumescent flame-retardant (IFR) system, and it exhibits excellent flame retarding efficiency for many polymers including EP.[4–8] However, some shortcomings of APP still exist in its application. APP can hardly perform well as a desirable IFR without a char-forming agent.[9] Moreover, the compatibility between APP and polymers is not very satisfactory.[10,11] To solve these problems, an extra carbonization agent and blowing agent were used to cover the shortage of the formation amount and intumescent degree of the char.[12–16] Pentaerythritol (PER) and melamine (MEL) are the most commonly used sources of charring and blowing agents, respectively. Surface modification of APP is an effective method to improve its compatibility in the polymer matrix.[17–23] However, the intumescent char layer of this APP-based IFR system is still not compact and dense; this makes its effect on fire control and smoke reduction less satisfactory. With respect to this issue, ferrocene,[12] iron oxide brown,[23] ferrite yellow,[24] montmorillonite,[25,26] melamine borate,[27] boric acid,[28] calcium borate,[29] titanium oxide,[30] zinc borate, and diantimony trioxide[31] were used to enhance the compactness and strength of the intumescent char. In our previous study, it has been found that Cu_2O exhibits better synergistic effect with epoxy-coated APP than other metal oxides, such as CuO, ZnO, SnO, Fe_2O_3, Ni_2O_3, and Co_2O_3, on the improvement of flame retardancy and smoke suppression of EP.[32] This was because Cu_2O was beneficial for the enhancement of the formation amount, intumescent degree, and compactness of char. The protective layer of intumescent char hindered the decomposition of EP and the diffusion of gaseous products, especially that of toxic gases. In addition, Cu_2O also played a role in the conversion of CO to CO_2 through a redox cycle.

School of Science (Sichuan), Xihua University, Chengdu 610039, China. E-mail: cmjchem@126.com; liuzg1964@163.com; Fax: +86-28-87720547; Tel: +86-28-87720547

In the past three years, note that a novel method for the modification of APP was developed by Wang's group.[33–39] This method was carried out by a cation exchange reaction between APP and organic amines. A series of APP-based organic–inorganic hybrids was prepared *via* amine replacement of the part of ammonia. Shao and Wang reported three monocomponent polymeric intumescent flame retardants, which were prepared by modifying APP with ethanediamine (EDA), ethanolamine (ETA), and piperazine (PA).[33–35] These modified APP exhibited excellent flame-retardant efficiency for polypropylene (PP). This study was further developed by Tan,[36–38] and diethylenetriamine- and polyethyleneimine-modified APP were prepared as multifunctional flame-retardant curing agents for EP. These curing agents not only improved the flame retardancy of EP, but also reduced the smoke emission. However, the curing temperature and time were higher than those needed in the common curing system[40–45] such as those involving 4,4′-diamino diphenyl methane (DDM) and polyamide (PA).

This study was conducted to explore whether the organic amine-modified APP acted as an additive type flame retardant and had a synergistic effect with Cu_2O on enhancing the flame retardancy and reducing the smoke release of EP. Herein, low molecular weight polyamide was chosen as the curing agent for EP, and ethanediamine-modified ammonium polyphosphate (EDA-APP) was used to build the monocomponent intumescent flame-retardant system. The contribution of EDA-APP to flame retardancy and smoke suppression was compared with that of APP, and the synergistic effect between EDA-APP and Cu_2O was investigated. In addition, the flame-retardant and smoke-suppressant mechanisms of EP/EDA-APP/Cu_2O composite were proposed by analyzing the gaseous and condensed pyrolysis products in detail.

2 Experimental

2.1 Materials

Bisphenol A epoxy with an epoxide equivalent of 5.1 mol kg^{-1} (commercial name E-51) was purchased from Nantong Xingchen Synthetic Material Co., Ltd., China. Although polyamide has the limitation of low heat resistance, it is still favorable to be used as a curing agent for epoxy because of its low toxicity, good compatibility, and toughening effect. Commercial polyamide (PA650) was obtained from Xiangtan Hongsang Viscose Materials Co., Ltd., China. The organic silicone antifoaming agent (AT86S) was supplied by Datian Chemical Co., Ltd., China. Commercial ammonium polyphosphate (APP, form II) was supplied by Shifang Taifeng New Flame Retardant Co., Ltd., China. Cuprous oxide (Cu_2O) and ethanediamine (EDA) were of analytical reagent grade and purchased from Chengdu Kelong Chemical Regent Factory, China.

2.2 Preparation of the epoxy composites

First, EDA-APP was prepared according to the previous research of Shao,[34] and the amount of EDA loaded into EDA-APP was about 4%. The chemical structure of EDA-APP is shown in Scheme 1. EDA-APP and Cu_2O were dried in a vacuum oven at 80 °C for 6 h before use. Then, E51, PA650 (curing agent), AT86S (antifoaming agent), EDA-APP (intumescent flame retardant), and Cu_2O (synergistic agent) were stirred at 60 °C until they were well blended. The mixture was then poured into preheated molds and cured at 120 °C for 2 h. The formulations of EP thermosets are listed in Table 1.

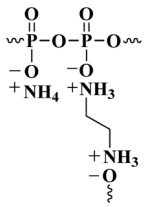

Scheme 1 The chemical structure of EDA-APP.

2.3 Measurements

Limiting oxygen index (LOI) value was determined at room temperature using a Jiangning JF-3 oxygen index instrument (China) according to ASTM D2863-97. The size of the specimen was 130 mm × 6.5 mm × 3.2 mm.

The UL-94 vertical burning test was performed using a Jiangning CZF-3 instrument (China) according to ASTM D3801. The dimension of the sample was 130 mm × 12.7 mm × 3.2 mm.

The flammability of the sample was measured by a FTT cone calorimeter instrument (UK) under a heat flux of 35 kW m^{-2} according to ISO 5660-1. The size of the specimen was 100 mm × 100 mm × 3 mm.

Thermogravimetric analysis (TGA) was performed using a Perkin-Elmer STA6000 instrument (UK). The sample (6–8 mg) was heated to 700 °C at a heating rate of 10 °C min^{-1} under a dynamic nitrogen flow of 50 mL min^{-1}.

Fourier transform infrared spectroscopy (FTIR) of the samples was performed using a Nicolet 380 spectrometer (US) in the wavenumber range from 500 to 4000 cm^{-1} using KBr pellets.

The gases evolved during the TGA tests were analyzed by coupling TG with FTIR. TGA and FTIR were performed using Perkin-Elmer STA6000 and FRONTIER instrument (UK), respectively. The samples were heated to 700 °C at a heating rate of 10 °C min^{-1} under a dynamic nitrogen flow of 50 mL min^{-1}.

The morphology of the char layers was observed by scanning electron microscopy (SEM). SEM images were obtained by an INSPECT F scanning electron microscope (US) at the accelerating voltage of 20 kV. The surfaces were coated with a thin gold layer before observation.

The phosphorus and copper contents of external and internal char layer were detected by energy-dispersive X-ray (EDX) spectroscopy (INCA, Oxford Instruments, Abingdon, Oxfordshire, U.K.).

3 Results and discussion

3.1 Fire performance

The flame retardancy of the epoxy composites was evaluated *via* LOI and UL-94 vertical burning tests, and the corresponding

Table 1 The formulations and flammability test (LOI and UL-94) data of epoxy composites

Sample	E51 (wt%)	PA 650 (wt%)	AT86S (wt%)	EDA-APP (wt%)	APP (wt%)	Cu_2O (wt%)	UL-94	LOI (%)
Neat EP	55.28	44.22	0.50				NR	20.0
EP/$APP_{25\%}$	41.39	33.11	0.50		25.00		V-0	35.0
EP/$APP_{21\%}$	43.61	34.89	0.50		21.00		NR	33.0
EP/$Cu_2O_{21\%}$	43.61	34.89	0.50			21.00	NR	22.0
EP/EDA-$APP_{21\%}$	43.61	34.89	0.50	21.00			V-0	33.0
EP/EDA-$APP_{20\%}$/$Cu_2O_{1\%}$	43.61	34.89	0.50	20.00		1.00	V-0	33.0
EP/EDA-$APP_{19\%}$/$Cu_2O_{2\%}$	43.61	34.89	0.50	19.00		2.00	V-0	33.5
EP/EDA-$APP_{18\%}$/$Cu_2O_{3\%}$	43.61	34.89	0.50	18.00		3.00	V-0	33.5
EP/EDA-$APP_{17\%}$/$Cu_2O_{4\%}$	43.61	34.89	0.50	17.00		4.00	V-1	32.5
EP/EDA-$APP_{16.3\%}$/$Cu_2O_{1.7\%}$	45.28	36.22	0.50	16.29		1.71	V-0	31.0
EP/EDA-$APP_{15.4\%}$/$Cu_2O_{1.6\%}$	45.83	36.67	0.50	15.38		1.62	V-1	30.5

data are summarized in Table 1. It illustrated that neat EP was a very flammable material because of its low LOI value (20%) and fast fire spread. The LOI value of EP can be improved to a certain extent *via* the incorporation of APP, Cu_2O, and EDA-APP. In addition, the highest UL-94 rating of V-0 can be reached through the introduction of APP and EDA-APP. However, to obtain V-0, the minimum demand for EDA-APP (21 wt%) was lower than that for APP (25 wt%). This indicated that EDA-APP was more effective than APP for enhancing the flame resistance of EP. To further improve the flame-retardant efficiency of EDA-APP, extra Cu_2O was added. The best mass ratio of EDA-APP to Cu_2O was determined to be 19 : 2 because EP/EDA-$APP_{19\%}$/$Cu_2O_{2\%}$ reached the highest LOI value of 33.5% and UL-94 rating of V-0. On controlling this mass ratio, the contents of EDA-APP can be further reduced to 16.3 wt% to reach V-0 and also to obtain the high LOI value of 31%. This indicated that Cu_2O had good synergistic effect with EDA-APP for the enhancement of the flame retardancy of EP.

Cone calorimeter measurement is one of the most effective methods for assessing the fire behavior of materials. Herein, it was used to analyze the flame retardancy, smoke suppression, and toxicity reduction of the flame-retardant EP composites. The heat release rate (HRR) and total heat release (THR) curves of neat EP, EP/$APP_{21\%}$, EP/EDA-$APP_{21\%}$, EP/$Cu_2O_{21\%}$, and EP/EDA-$APP_{19\%}$/$Cu_2O_{2\%}$ are shown in Fig. 1. The corresponding data obtained from cone calorimetry are presented in Table 2. From Fig. 1, it can be seen that both the HRR and THR of EP composites were obviously reduced *via* the addition of any kind of additives (APP, EDA-APP, and Cu_2O) as compared to those of neat EP. In Table 2, note that the contribution of EDA-APP was much better than that of APP towards the reduction of the peak of the heat release rate (PHRR) for EP. In addition, EDA-APP also exhibited better performance than APP on increasing the time to ignition (TTI) and time to PHRR (t_P), as well as on decreasing the average heat release rate (AvHRR), fire growth rate (FIGRA), and maximum average rate of heat emission (MARHE). This illustrated that the fire risk of the EP/EDA-$APP_{21\%}$ system was greatly lower than that of the EP/$APP_{21\%}$ system. With the purpose of further improving the flame retardancy of the EP/EDA-APP system, Cu_2O was added to it. The results showed that the PHRR and AvHRR of EP/EDA-$APP_{19\%}$/$Cu_2O_{2\%}$ were declined by about 68% and 61%, *i.e.* to 364 kW m^{-2} and 65 kW m^{-2}, respectively, only *via* the addition of extra 2 wt% Cu_2O. Moreover, the compactness of the char layer was obviously enhanced by Cu_2O because of the absence of holes and cracks, as shown in Fig. 2.

3.2 Suppression of the smoke and toxic gases

It has been reported that most fire deaths are due to smoke inhalation, oxygen deprivation, and toxic gases instead of

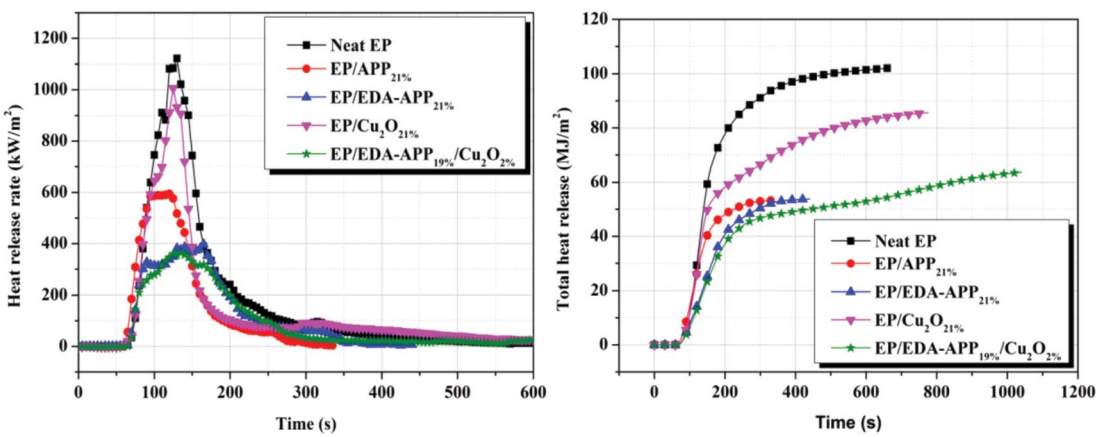

Fig. 1 The heat release rate and total heat release curves of neat EP, EP/$APP_{21\%}$, EP/EDA-$APP_{21\%}$, EP/$Cu_2O_{21\%}$, and EP/EDA-$APP_{19\%}$/$Cu_2O_{2\%}$.

Table 2 The data of cone calorimeter test on neat EP and EP composites with 21 wt% of flame retardants[a]

Sample	TTI (s)	PHRR (kW m^{-2})	AvHRR (kW m^{-2})	t_P (s)	FIGRA	THR (MJ m^{-2})	MARHE (kW m^{-2})
Neat EP	53	1121	167	130	8.62	102	408
EP/APP$_{21\%}$	57	594	194	120	4.95	53	269
EP/EDA-APP$_{21\%}$	61	398	144	165	2.40	54	203
EP/$Cu_2O_{21\%}$	47	1007	118	125	8.06	86	331
EP/EDA-APP$_{19\%}$/$Cu_2O_{2\%}$	62	364	65	135	2.70	64	186

[a] TTI means time to ignition, PHRR represents the peak of heat release rate, AvHRR is the average heat release rate, t_P denotes time to PHRR, FIGRA is calculated by dividing the PHRR by t_P, THR represents total heat release, and MARHE denotes the maximum average rate of heat emission.

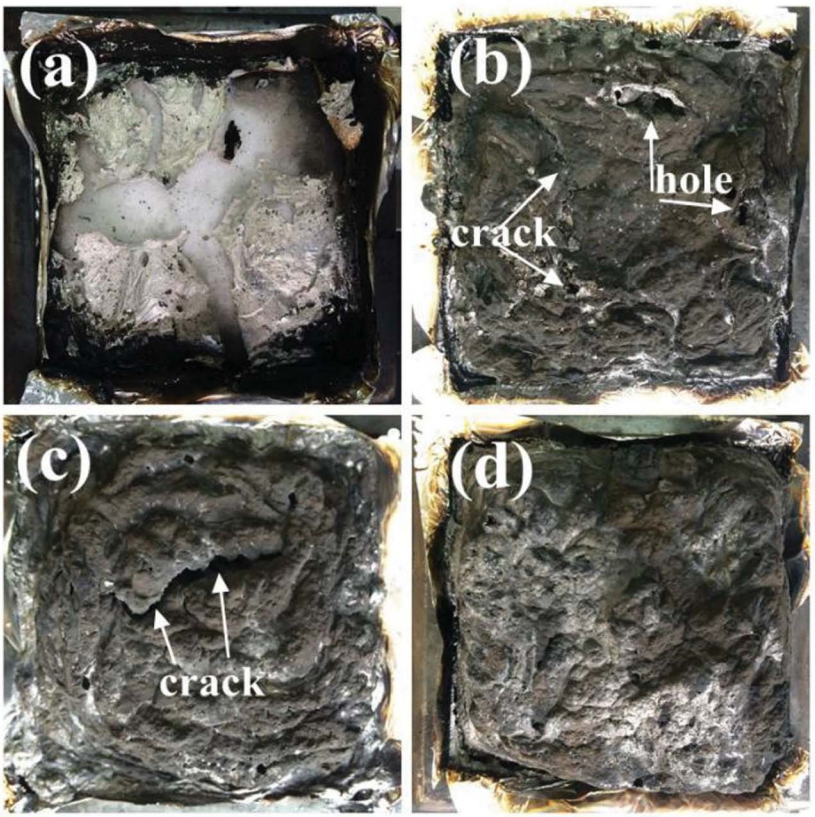

Fig. 2 The images for char residues of neat EP (a), EP/APP$_{21\%}$ (b), EP/EDA-APP$_{21\%}$ (c), and EP/EDA-APP$_{19\%}$/$Cu_2O_{2\%}$ (d) after cone calorimeter test.

burns.[3] The disadvantages of EP are not only its high flammability, but also the large amount of dense smoke and toxic gases generated during its combustion. Obviously, smoke production rate (SPR), total smoke production (TSP), and CO production (COP) are important parameters for assessing the fire hazard of EP. It can be observed from Fig. 3 that the SPR of EP/EDA-APP$_{21\%}$ was lower than that of EP/APP$_{21\%}$, and the addition of Cu_2O further reduced the SPR and TSP of the EP/EDA-APP composite. Furthermore, the CO production (COP) and CO_2 production (CO_2P) were also decreased upon the loading of Cu_2O into the EP/EDA-APP composite, as shown in Fig. 4. Especially, the COP of EP/EDA-APP$_{19\%}$/$Cu_2O_{2\%}$ was lessened by 53% as compared to that of neat EP. It was probably due to the enhancement of the char formation amount and the intumescent degree caused by Cu_2O, as well as the catalytic oxidation action of Cu_2O on CO.

To further understand the composition of the smoke, TG coupled with FTIR (TG-FTIR) was used to determine the pyrolysis products of neat EP, EP/APP$_{21\%}$, and EP/EDA-APP$_{21\%}$. The absorbance of four characteristic gaseous products, *i.e.* ammonia (NH_3), hydrocarbons, aromatic compounds, and epoxy derivatives, are shown in Fig. 5. It can be seen that the addition of APP and EDA-APP caused the increase of NH_3, but decrease of hydrocarbons, aromatic compounds, and epoxy derivatives. In addition, more NH_3 was released from EP/APP$_{21\%}$ than EP/EDA-APP$_{21\%}$. However, EP/EDA-APP$_{21\%}$ was better than EP/APP$_{21\%}$ in restraining the production of hydrocarbons, aromatic compounds, and epoxy derivatives. This is

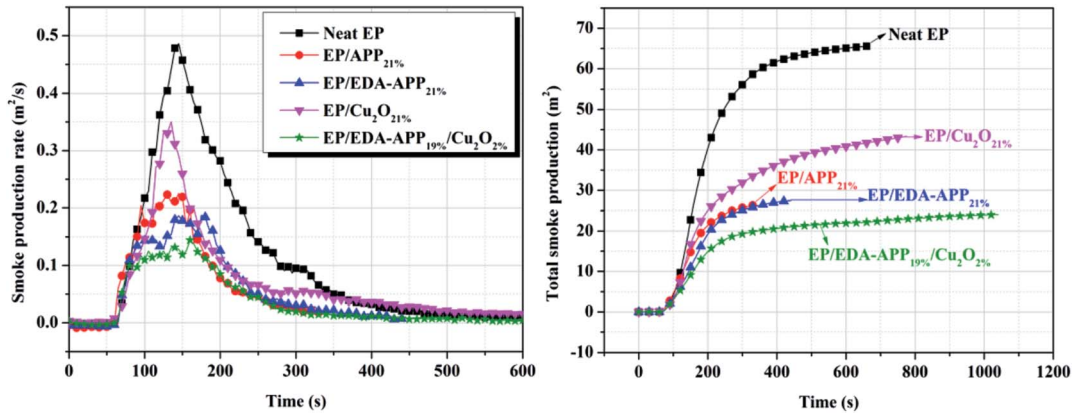

Fig. 3 The smoke production rate and total smoke production curves of neat EP, EP/$APP_{21\%}$, EP/EDA-$APP_{21\%}$, EP/$Cu_2O_{21\%}$, and EP/EDA-$APP_{19\%}$/$Cu_2O_{2\%}$.

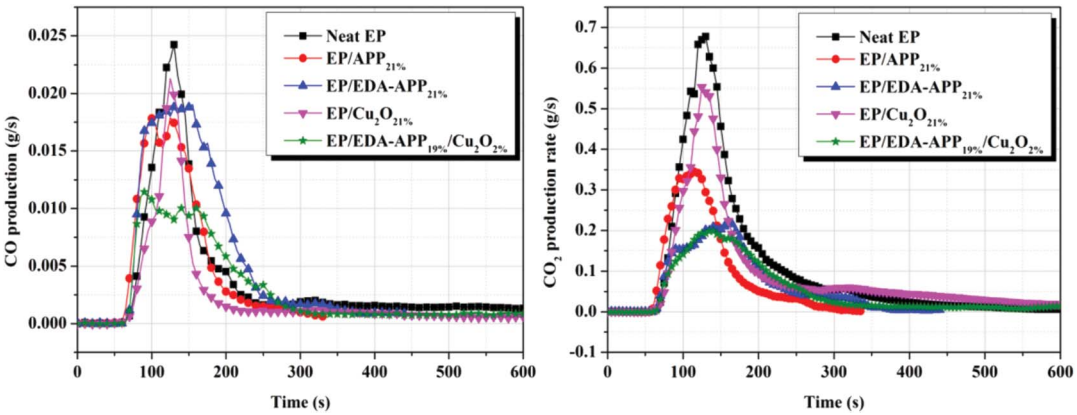

Fig. 4 The CO and CO_2 production curves of neat EP, EP/$APP_{21\%}$, EP/EDA-$APP_{21\%}$, EP/$Cu_2O_{21\%}$, and EP/EDA-$APP_{19\%}$/$Cu_2O_{2\%}$.

due to the fact that an ammonium group of EDA-APP was substituted by ethanediamine; this led to the reduction of NH_3, but improvement of the char formation rate for EP/EDA-$APP_{21\%}$. The initially formed intumescent char was in favor of hindering the decomposition of EP and suppressing the release of smoke and toxic gases.

3.3 Thermal degradation analysis

The thermal degradation behaviors of APP, EDA-APP, neat EP, and EP composites with 21 wt% of flame retardants (APP, EDA-APP, and Cu_2O) were investigated by TGA. The TG and DTG curves of them are presented in Fig. 6, and the main results are summarized in Table 3. It can be observed from Fig. 6 that both APP and EDA-APP contain two weak (300–450 °C) and one strong (450–650 °C) weight loss processes. The degradation in the range of 300–450 °C was mainly due to the elimination of NH_3 and H_2O, and the weight loss at 450–650 °C was attributed to the pyrolysis of phosphoric acid and its derivatives.[46] The weight loss rate of EDA-APP was lower than that of APP before 620 °C but became higher after 620 °C. The reason was that the C–N (305 kJ mol^{-1}) bond of ethanediamine salt (NH_3^+–CH_2–CH_2–NH_3^+) in EDA-APP was less stable than the P–O (335 kJ mol^{-1}) bond in APP.[36,47] This also caused the decrease in the initial degradation temperature ($T_{5\%}$) of EDA-APP. The early decomposition of EDA-APP helped in the generation of phosphoric acid and its derivatives in advance that acted as dehydrating agents for carbonization. Thus, EDA-APP produced a stable char residue earlier than APP, and as a result, more char residue was formed. Moreover, these phosphoric acid derivatives generated from EDA-APP promoted the dehydration of EP and the formation of protective char earlier than APP. This was the reason for the lower weight loss rate of EP/EDA-$APP_{21\%}$ than that of EP/$APP_{21\%}$ in the range of 300–400 °C. When Cu_2O was added to the EP/EDA-APP system, the decomposition of EP was accelerated, and the char residue was improved.

3.4 Flame-retardant and smoke-suppressant mechanisms

To evaluate how EDA-APP worked on improving the flame retardancy of EP and how EDA-APP/Cu_2O acted on suppressing the release of smoke and toxic gases, the condensed phase and gaseous phase pyrolysis products of EDA-APP were investigated by FTIR (Fig. 7). The condensed phase decomposition products of EDA-APP were obtained in a muffle furnace. The gaseous products of EDA-APP, neat EP, and EP/EDA-$APP_{21\%}$ evolved

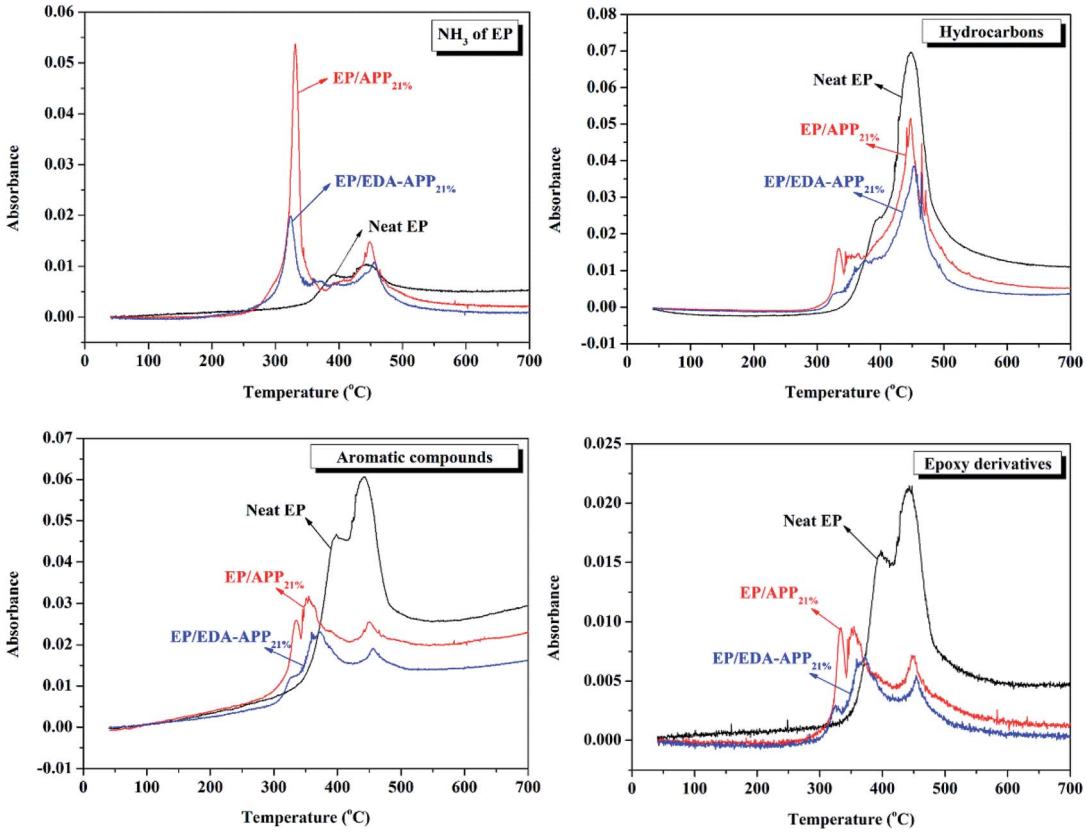

Fig. 5 Intensity of characteristic peaks for NH_3, hydrocarbons, aromatic compounds, and epoxy derivatives pyrolysised from Neat EP, EP/$APP_{21\%}$, and EP/EDA-$APP_{21\%}$.

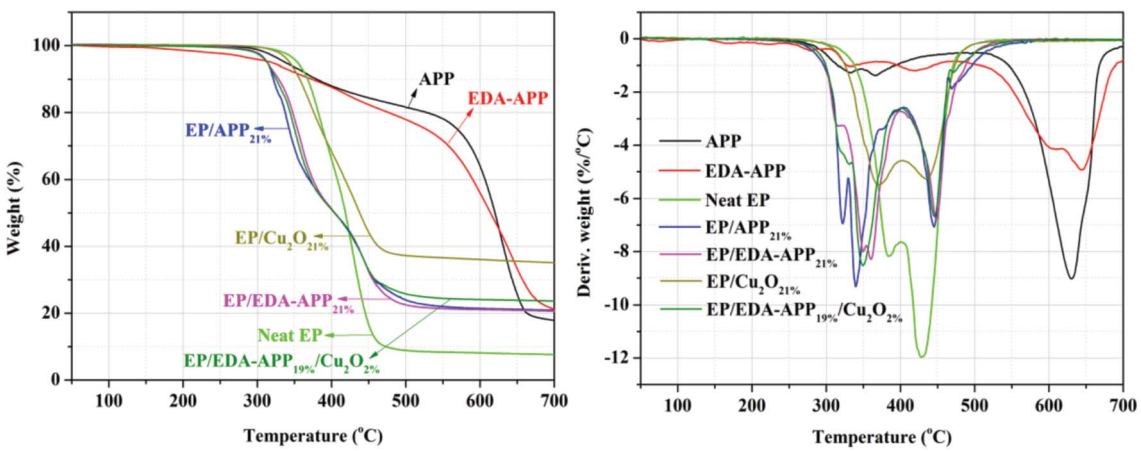

Fig. 6 TG and DTG curves of APP, EDA-APP, neat EP, and EP composites with 21 wt% of flame retardants at the heating rate of 10 °C min^{-1} in N_2.

during TGA tests were analyzed by coupling TG with FTIR, as shown in Fig. 7 and 8. The microstructure and composition of the chars of EP/EDA-$APP_{19\%}$/$Cu_2O_{2\%}$ after the cone calorimeter test were examined by SEM and EDX (Fig. 9).

From Fig. 7, it can be observed that NH_2 group (3435, 3336 cm^{-1}), NH_3^+ group (3201 cm^{-1}), NH_4^+ group (3126 cm^{-1}), CH_2 group (2921, 2852 cm^{-1}), P═O group (1250 cm^{-1}), and P–O group (1069 cm^{-1}) existed in EDA-APP. With the beginning of decomposition, the NH_2 and NH_3^+ groups broke at about 315 °C, the NH_4^+, P═O, and P–O groups were gradually weakened before 420 °C, and the concomitant products were NH_3 (964 and 930 cm^{-1}), H_2O (3126 cm^{-1}), and a small amount of gases containing P═O (1249 cm^{-1}), P–H (2362 cm^{-1}), C═C (1629 cm^{-1}), and C≡N (2240 cm^{-1}) groups. At a higher temperature (644 °C), NH_4^+ was ruptured absolutely and there was no NH_3 emission. However, a stable char residue with C═C

Table 3 TGA data of APP, EDA-APP, neat EP, and EP composites with 21 wt% of flame retardants at the heating rate of 10 °C min^{-1} in N_2

Sample	$T_{5\%}$[a] (°C)	T_{max1}[b] (°C)	T_{max2} (°C)	T_{max3} (°C)	wt_R^{700}[c] (%)
APP	336	332	365	630	18
EDA-APP	315	334	420	644	21
Neat EP	352	382	428		7
$EP/APP_{21\%}$	312	321	339	444	21
$EP/EDA\text{-}APP_{21\%}$	311	359	447		20
$EP/Cu_2O_{21\%}$	343	369	434		35
$EP/EDA\text{-}APP_{19\%}/Cu_2O_{2\%}$	311	347	445		24

[a] $T_{5\%}$ denotes the temperature at 5% weight loss. [b] T_{max1} denotes the temperature at the first maximum weight loss. [c] wt_R^{700} denotes the weight of char residue at 700 °C.

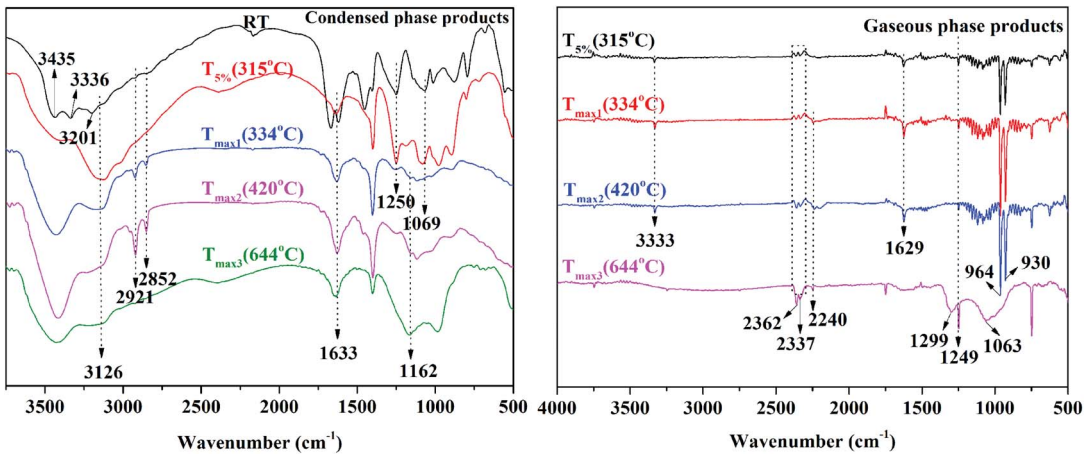

Fig. 7 The FTIR spectra of condensed and gaseous phase pyrolysis products of EDA-APP at different temperatures.

or C=N (1633 cm^{-1}) and P–N–C group (1162 cm^{-1}) was formed; moreover, the gases containing the P=O, P–O (1063 cm^{-1}), and P–H groups were increased. It indicated that the elimination of NH_3 and H_2O mainly occurred before 420 °C, and the majority of phosphoric acid and its derivatives were produced after this temperature.

Fig. 8 shows the FTIR spectra of gaseous products of neat EP and $EP/EDA\text{-}APP_{21\%}$. A large amount of harmful gases containing aromatic compounds (3015 and 1508 cm^{-1}), hydrocarbons (2973, 2935, and 2878 cm^{-1}), and epoxy derivatives (827, 749 cm^{-1}) were diffused during the decomposition of neat EP. The loading of EDA-APP caused the enhancement of the peaks at 2360 and 2230 cm^{-1}; moreover, a lot of NH_3 was generated at 964 and 930 cm^{-1}. This was due to the stretching vibration of some gases containing P–H group that appeared near 2360 cm^{-1}. The generation of NH_3 was derived from EDA-APP.

The morphology and composition of the external and internal chars of $EP/EDA\text{-}APP_{19\%}/Cu_2O_{2\%}$ are shown in Fig. 9. The external char layer was so compact and dense (Fig. 9(a) and (b)) that it effectively hindered the transmission of heat and oxygen from the flame zone to the surface of the material. A swollen char layer (Fig. 9(c) and (d)) was formed on the internal surface, which effectively prevented the inside pyrolysis products from transmitting into the flame zone. The elements such as carbon (C), nitrogen (N), oxygen (O), phosphorus (P), and copper (Cu) were found in the external and internal char layer (Fig. 9(e) and (f)), and their average weight percentage were found to be 39.06 wt%, 42.72 wt%, 12.83 wt%, 3.38 wt%, and 2.01 wt%, respectively. Interestingly, the nitrogen content of the external char layer was higher than that of the internal char layer; on the contrary, the phosphorus content of the internal char layer was higher. It illustrated that the external char surface was mainly composed of the nitrogen-containing stable char layer, and the phosphorus-rich char mainly remained on the internal surface. This intumescent char layer was composed of products containing alkyl groups (2918 and 2855 cm^{-1}), C=C, C=N, N=N, and aryl groups (1633 cm^{-1}), P=O group (1262 cm^{-1}), P–N–C group (1144 cm^{-1}), and P–O group (1080 cm^{-1}), as shown in Fig. 9(g). Cu_2O in the EP/EDA-APP composite was finally oxidized to CuO, which was uniformly dispersed in the char and acted as a good synergist for enhancing the compactness of the EP/EDA-APP char residue. The most possible constituents and the corresponding element contents of char residue are listed in Table 4.

On combining the abovementioned results with the reported findings,[34,37,38] the possible flame-retardant and smoke-suppressant mechanisms are proposed in Scheme 2. The early decomposition of EDA-APP caused the generation of phosphoric acid and its derivatives in advance (before 450 °C), which was beneficial to promote the dehydration of EP and the earlier formation of protective char. In addition, Cu_2O further

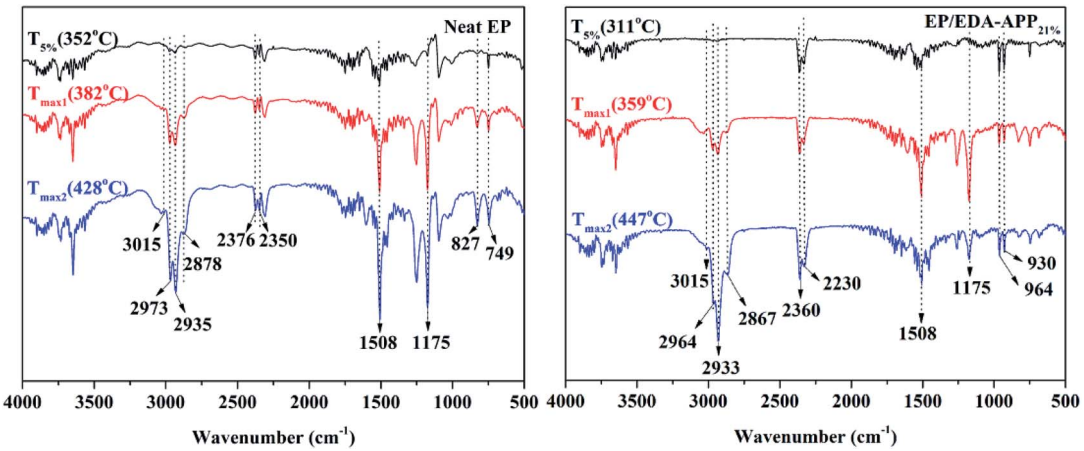

Fig. 8 The FTIR spectra of gaseous phase pyrolysis products of neat EP and EP/EDA-APP$_{21\%}$ during TGA in a N_2 atmosphere.

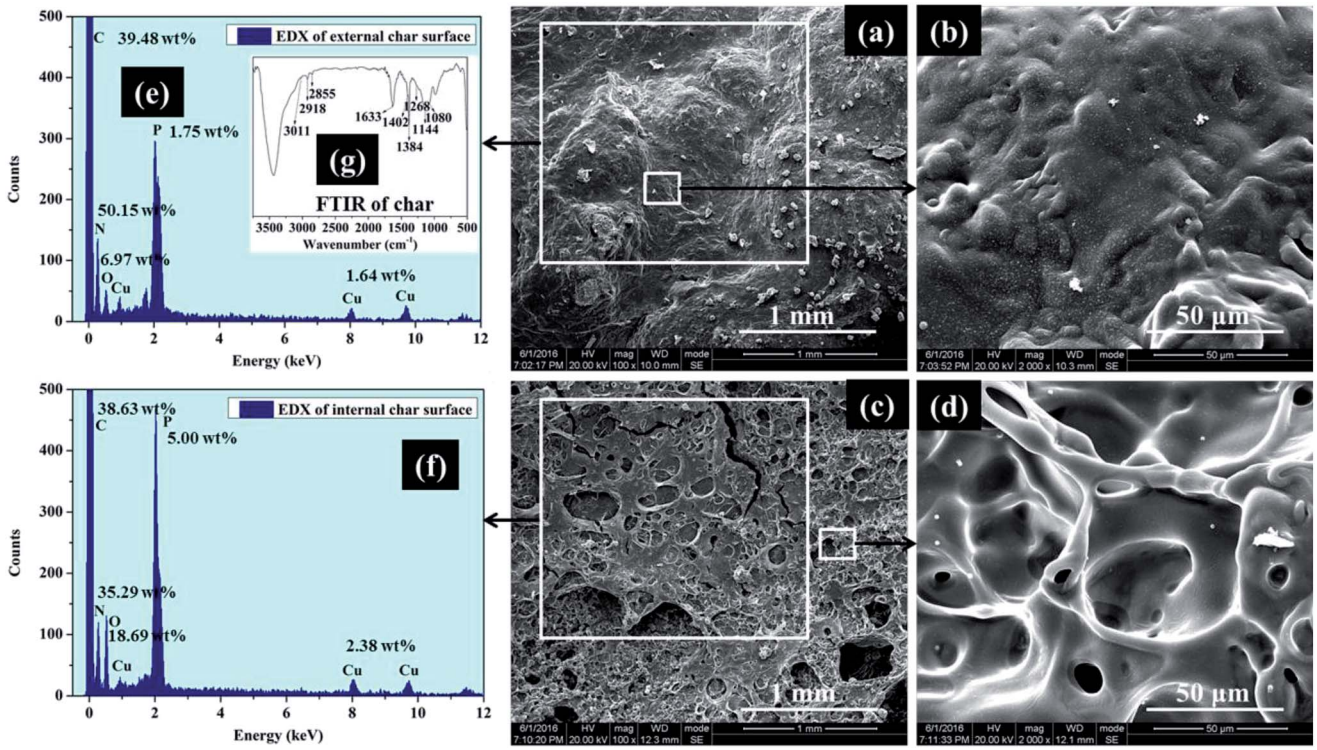

Fig. 9 SEM microphotographs and EDX spectra of external and internal char layers of EP/EDA-APP$_{19\%}$/$Cu_2O_{2\%}$ after cone calorimeter test.

Table 4 The most possible constituents and the corresponding element contents

Constituents	C (wt%)	N (wt%)	O (wt%)	P (wt%)	Cu (wt%)
CuO			0.50		2.01
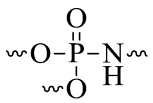		1.53	5.23	3.38	
Ph–O–			7.1		
C=N, N=N		41.19			
C=C, aryl, alkyl	39.06				
Total	39.06	42.72	12.83	3.38	2.01

accelerated the decomposition of EDA-APP and EP. These helped in the improvement of the char formation rate. An early formed intumescent char was a barrier that prevented heat and O_2 to transmit into the matrix, hindering the combustible gases feed back into the flame zone and subsequently suppressing the release of smoke and toxic gases. Furthermore, Cu_2O not only played a role in the oxidation of CO, but also exhibited good synergistic effect with EDA-APP for improving the formation amount, intumescent degree, and compactness of char.

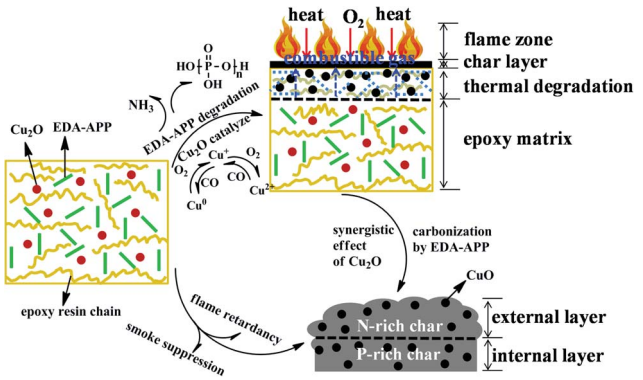

Scheme 2 The possible flame-retardant and smoke-suppressant mechanisms of the EP/EDA-APP/Cu_2O composite.

4 Conclusions

In conclusion, flame-retardant EP composites were prepared using EDA-APP as an intumescent flame retardant and Cu_2O as a synergist. LOI and UL-94 test results showed that the minimum demand of EDA-APP was lower than that of APP to obtain UL-94 V-0 rating. The flame-retardant efficiency of the EP/EDA-APP system can be enhanced *via* the addition of extra Cu_2O. In addition, cone calorimeter and TG-FTIR test results indicated that Cu_2O had synergistic effect with EDA-APP for suppressing the emission of smoke and toxic gases such as carbon monoxide, hydrocarbons, aromatic compounds, and epoxy derivatives. After analyzing the thermal decomposition behavior of EDA-APP and EP/EDA-APP composites and the composition of their gaseous and condensed pyrolysis products, the flame-retardant and smoke-suppressant mechanisms of EP/EDA-APP/Cu_2O composite were proposed. It was deduced that EDA-APP was earlier than APP in producing stable char residue, and the formation amount, intumescent degree, and compactness of the char were further improved because of the synergistic effect and catalytic action of Cu_2O.

Acknowledgements

This work was financially supported by the National Natural Science Foundation of China (21504071), the Opening Project of State Key Laboratory of Polymer Materials Engineering of Sichuan University (sklpme2015-4-34), and the Open Research Subject of Key Laboratory of Automobile High Performance Materials & Forming Technology in Sichuan Provincial Universities (szjj2015-091 and szjj2016-053).

References

1 R. Oliwa, M. Heneczkowski, M. Oleksy and H. Galina, *Composites, Part B*, 2016, **95**, 1–8.
2 N. Saba, M. Jawaid, M. T. Paridah and O. Y. Al-othman, *Polym. Adv. Technol.*, 2016, **27**, 577–590.
3 D. J. Irvine, J. A. McCluskey and I. M. Robinson, *Polym. Degrad. Stab.*, 2000, **67**, 383–396.
4 J. Alongi, Z. Han and S. Bourbigot, *Prog. Polym. Sci.*, 2015, **51**, 28–73.
5 H. Q. Qu, W. H. Wu, J. W. Hao, J. H. Sun and J. Z. Xu, *J. Macromol. Sci., Phys.*, 2013, **53**, 278–295.
6 W. K. Patrick Lim, M. Mariatti, W. S. Chow and K. T. Mar, *Composites, Part B*, 2012, **43**, 124–128.
7 R. G. Puri and A. S. Khanna, *J. Coat. Technol. Res.*, 2016, **14**, 1–20.
8 Y. Zhang, B. Wang, H. Sheng, B. Yuan, B. Yu, G. Tang, G. Jie, H. Feng, Y. Tao and Y. Hu, *RSC Adv.*, 2016, **6**, 85564–85573.
9 L. Boccarusso, L. Carrino, M. Durante, A. Formisano, A. Langella and F. M. C. Minutolo, *Composites, Part B*, 2016, **89**, 117–126.
10 M. Hesami, R. Bagheri and M. Masoomi, *Iran. Polym. J.*, 2014, **23**, 469–476.
11 P. F. Chen, F. Zhang, S. X. Li and Y. F. Cheng, *J. Appl. Polym. Sci.*, 2016, **133**, 43912–43917.
12 L. Liu, X. Chen and C. Jiao, *J. Therm. Anal. Calorim.*, 2015, **122**, 437–447.
13 L. Liu, X. Chen and C. Jiao, *Iran. Polym. J.*, 2015, **24**, 337–347.
14 K. Zhang, K. Wu, Y. K. Zhang, H. F. Liu, M. M. Shen and W. Hu, *Polym.-Plast. Technol. Eng.*, 2013, **52**, 525–532.
15 S. Zhang, F. Liu, H. Peng, X. Peng, S. Jiang and J. Wang, *Ind. Eng. Chem. Res.*, 2015, **54**, 11944–11952.
16 W. Y. Gao, S. J. Wang, F. B. Meng, Y. H. Wang and H. Q. Ma, *J. Appl. Polym. Sci.*, 2016, **133**, 43720–43727.
17 W. Gao, S. Wang, H. Ma, Y. Wang and F. Meng, *J. Phys. Chem. C*, 2015, **119**, 28999–29005.
18 Z. Jiang and G. Liu, *RSC Adv.*, 2015, **5**, 88445–88455.
19 F. Luo, K. Wu, M. Lu, S. Nie, X. Li and X. Guan, *J. Therm. Anal. Calorim.*, 2015, **120**, 1327–1335.
20 H. Qu, W. Wu, J. Hao, C. Wang and J. Xu, *Fire Mater.*, 2014, **38**, 312–322.
21 I. Vroman, S. Giraud, F. Salaün and S. Bourbigot, *Polym. Degrad. Stab.*, 2010, **95**, 1716–1720.
22 L. Yang, W. Cheng, J. Zhou, H. Li, X. Wang, X. Chen and Z. Zhang, *Polym. Degrad. Stab.*, 2014, **105**, 150–159.
23 X. Chen, L. Liu and C. Jiao, *Adv. Polym. Technol.*, 2015, **34**, 21516–21524.
24 X. Chen, Y. Jiang and C. Jiao, *J. Hazard. Mater.*, 2014, **266**, 114–121.
25 X. He, W. Zhang, D. Yi and R. Yang, *J. Fire Sci.*, 2016, **34**, 212–225.
26 W. Zhang, X. He, T. Song, Q. Jiao and R. Yang, *Polym. Degrad. Stab.*, 2015, **112**, 43–51.
27 B. Schartel, A. Weiß, F. Mohr, M. Kleemeier, A. Hartwig and U. Braun, *J. Appl. Polym. Sci.*, 2010, **118**, 1134–1143.
28 M. Jimenez, S. Duquesne and S. Bourbigot, *Surf. Coat. Technol.*, 2006, **201**, 979–987.
29 W. P. Lim, M. Mariatti, W. Chow and K. Mar, *J. Fire Sci.*, 2012, **30**, 428–436.
30 H. Aziz and F. Ahmad, *Prog. Org. Coat.*, 2016, **101**, 431–439.
31 F. Zhang, P. Chen, Y. Wang and S. Li, *J. Therm. Anal. Calorim.*, 2015, **123**, 1319–1327.
32 M. J. Chen, Y. C. Lin, X. N. Wang, L. Zhong, Q. L. Li and Z. G. Liu, *Ind. Eng. Chem. Res.*, 2015, **54**, 12705–12713.

33 Z. B. Shao, C. Deng, Y. Tan, M. J. Chen, L. Chen and Y. Z. Wang, *ACS Appl. Mater. Interfaces*, 2014, **6**, 7363–7370.
34 Z. B. Shao, C. Deng, Y. Tan, M. J. Chen, L. Chen and Y. Z. Wang, *Polym. Degrad. Stab.*, 2014, **106**, 88–96.
35 Z. B. Shao, C. Deng, Y. Tan, L. Yu, M. J. Chen, L. Chen and Y. Z. Wang, *J. Mater. Chem. A*, 2014, **2**, 13955–13965.
36 Y. Tan, Z. B. Shao, X. F. Chen, J. W. Long, L. Chen and Y. Z. Wang, *ACS Appl. Mater. Interfaces*, 2015, **7**, 17919–17928.
37 Y. Tan, Z. B. Shao, L. X. Yu, J. W. Long, M. Qi, L. Chen and Y. Z. Wang, *Polym. Chem.*, 2016, **7**, 3003–3012.
38 Y. Tan, Z. B. Shao, L. X. Yu, Y. J. Xu, W. H. Rao, L. Chen and Y. Z. Wang, *Polym. Degrad. Stab.*, 2016, **131**, 62–70.
39 S. F. Liao, C. Deng, S. C. Huang, J. Y. Cao and Y. Z. Wang, *Chin. J. Polym. Sci.*, 2016, **34**, 1339–1353.
40 D. Balgude, A. Sabnis and S. K. Ghosh, *Prog. Org. Coat.*, 2017, **104**, 250–262.
41 P. Deepak, R. Vignesh Kumar, S. Badrinarayanan, H. Sivaraman and R. Vimal, *Mater. Today*, 2017, **4**, 2841–2850.
42 S. D. Jiang, Z. M. Bai, G. Tang, Y. Hu and L. Song, *Ind. Eng. Chem. Res.*, 2014, **53**, 6708–6717.
43 J. D. McCoy, W. B. Ancipink, C. M. Clarkson, J. M. Kropka, M. C. Celina, N. H. Giron, L. Hailesilassie and N. Fredj, *Polymer*, 2016, **105**, 243–254.
44 P. Müller, M. Morys, A. Sut, C. Jäger, B. Illerhaus and B. Schartel, *Polym. Degrad. Stab.*, 2016, **130**, 307–319.
45 W. Zhang, X. Li, H. Fan and R. Yang, *Polym. Degrad. Stab.*, 2012, **97**, 2241–2248.
46 G. S. Liu, W. Y. Chen and J. G. Yu, *Ind. Eng. Chem. Res.*, 2010, **49**, 12148–12155.
47 M. J. Xu, W. Zhao and B. Li, *J. Appl. Polym. Sci.*, 2014, **131**, 41159–41170.